The following publication Q. Zhang et al., "Algorithms for Blind Separation and Estimation of Transmitter and Receiver IQ Imbalances," in Journal of Lightwave Technology, vol. 37, no. 10, pp. 2201-2208, 15 May, 2019 is available at https://doi.org/10.1109/JLT.2019.2899833.

Algorithms for Blind Separation and Estimation of Transmitter and Receiver IQ Imbalances

Qun Zhang, Yanfu Yang, Changjian Guo, Xian Zhou, Yong Yao, Alan Pak Tao Lau, and Chao Lu

***Abstract*—We propose a blind transmitter (Tx) and receiver (Rx) in-phase/quadrature (IQ) amplitude and phase imbalances estimation scheme based on a combination of analytical modelling and clustering algorithms. The proposed scheme can isolate and separately estimate Tx and Rx phase and amplitude imbalances, applicable to high-order multi-modulus signals, and hence is a great physical-layer-monitoring tool for network disaggregation. We first estimate the Rx imbalances by identifying the fact that the received signal distribution in presence of laser frequency offset (FO), phase noise (PN) and Rx imbalance forms concentric ellipses. A convex hull assisted ellipse correction (EC) algorithm is used to determine the Rx IQ imbalance parameters that best match the ellipses. Standard laser FO compensation algorithm follows. A *k*-means clustering assisted blind phase search (BPS) algorithm is then employed to mitigate the PN in presence of Tx imbalances. Finally, another iterative *k*-means clustering procedure is used to estimate the Tx IQ imbalances. The proposed scheme is evaluated experimentally for 34 Gbaud QPSK and 16-QAM signals. The accurate estimation for a wide range of Tx and Rx IQ imbalances and good robustness to amplified spontaneous emission (ASE) noise is demonstrated.**

***Index Terms*—Optical fiber communication, digital signal processing, parameter estimation, machine learning.**

I. Introduction

Coherent detection and digital signal processing (DSP) are now extensively adopted in long haul and metro optical networks. Meanwhile, coherent detection is also considered as a promising technology to implement beyond 400G datacenter interconnects (DCI). IQ amplitude and phase imbalances are important impairments in coherent optical transceivers [1], which can cause serious system performance degradation, especially when high order modulations are used. In a typical IQ modulator based-Tx implementation, the IQ amplitude imbalance refers to the amplitude difference between the I and Q components applied on the modulator due to the electrical amplifier or electro-optical response mismatch. The IQ phase imbalance refers to the phase deviation from $\pi/2$ between the I and Q tributaries of the IQ modulator, which may result from un-stable bias control [2]. At the Rx, the IQ amplitude imbalance arises from the mismatch of the photodetectors (PD) as well as the transimpedance amplifiers (TIA). Meanwhile, the IQ phase imbalance may be caused by the phase deviation from $\pi/2$ in the optical hybrid [3]. The specifications of the IQ imbalances for 100-Gb/s coherent optical interfaces are also actively investigated in a revision of ITU-T G.698.2. However, legacy aggregated network vendors provide highly integrated networking solutions and make it difficult to single out and locate physical layer issues at Tx or Rx. As the optical networking community is moving towards network disaggregation, it is therefore crucial to develop methodologies to isolate and examine the performance of individual components from received signals.

To this end, various algorithms were proposed to compensate the IQ imbalances, including Gram-Schmidt orthogonalization procedure (GSOP) [4], EC [5] and adaptive filtering algorithms [6]-[12]. The GSOP method is used to whiten the received signal and construct a new orthonormal signal according to statistics information. But GSOP is only applicable to the compensation of Rx IQ imbalances and is inefficient in compensating Tx IQ imbalances [13]. EC is used to fit the ellipse curve according to the least square (LS) method. However, EC can not be used to compensate the Tx IQ imbalances and is not appropriate to multi-modulus signals [14]. The adaptive filtering based algorithms can be used to compensate both the Tx or Rx IQ imbalances. However, extra training symbols are needed for estimation of the imbalances [12].

The above-mentioned algorithms mainly focus on the compensation of either Tx or Rx side IQ imbalances. However, there are currently few algorithms that can estimate both Tx and Rx IQ imbalances without training data. Therefore, in this work

This work was supported by the National Natural Science Foundation of China (Contract No. 61435006, 61671053), Shenzhen Municipal Science and Technology Plan Project (JCYJ20150529114045265), Pearl River S&T Nova Program of Guangzhou (201710010028), Hong Kong Government General Research Fund under project number PolyU 152757/16E, 152248/15E, Hong Kong Polytechnic University Project G-YBPH, and Huawei project PolyU H-ZG5L. (*Corresponding Authors: Yanfu Yang and Changjian Guo*.)

Q. Zhang is with the Harbin Institute of Technology, Shenzhen, China. He is also with South China Normal University, Guangzhou, China, and the Hong Kong Polytechnic University, Hong Kong. (e-mail: 16b958076@stu.hit.edu.cn).

Y. Yang and Y. Yao is with the Department of Electronic and Information Engineering, Harbin Institute of Technology, Shenzhen, China (e-mail: yangyanfu@hit.edu.cn; yaoyong@hit.edu.cn).

C. Guo is with South China Academy of Advanced Optoelectronics, South China Normal University, Guangzhou 510006, China (e-mail: changjian.guo@coer-scnu.org).

X. Zhou and C. Lu are with the Department of Electronic and Information Engineering, Hong Kong Polytechnic University, Hong Kong (e-mail: xian.zhou@polyu.edu.hk; chao.lu@polyu.edu.hk).

A. P. T. Lau is with the Department of Electrical Engineering, Hong Kong Polytechnic University, Hong Kong (e-mail: eeaptlau@polyu.edu.hk).

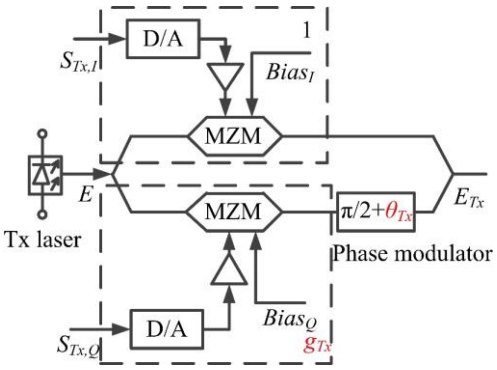

Fig. 1. Block diagram of the transmitter (Tx).

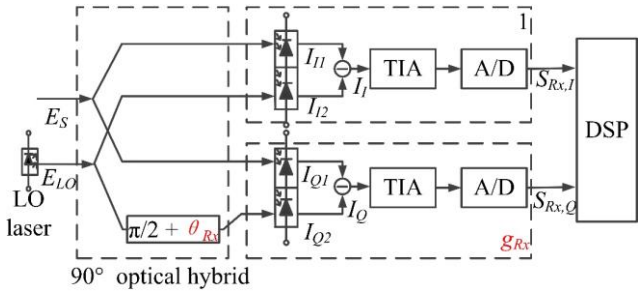

Fig. 2. Block diagram of the Receiver (Rx).

we propose a blind estimation scheme for IQ imbalances of both Tx and Rx based on machine learning in coherent optical communication systems. In our proposed scheme, the Rx and Tx IQ imbalances are estimated using a convex hull assisted EC algorithm and a *k*-means assisted BPS algorithm, respectively, according to their different impacts on the received signal. The models of Tx and Rx are analyzed in presence of IQ imbalances. The proposed algorithm is tested on 34 Gbaud QPSK and 16QAM modulated coherent optical systems. The experiment results show that the proposed algorithm can respectively estimate Tx and Rx amplitude IQ imbalances ranged from -7 dB to 7 dB within 1 dB of estimation error. The proposed algorithm can respectively estimate Tx and Rx phase IQ imbalances ranged from -80 degrees to 80 degrees within 4 degrees of estimation error.

The rest of the paper is organized as follows. The mathematical models of Tx and Rx in the presence of IQ imbalances are given in section II. The impacts of Tx and Rx IQ imbalances on the received signals after coherent detection are analyzed in section III. The principle of the proposed estimating algorithm is described in section IV. In order to facilitate the analysis of the impact of different impairment, the results displayed in section III and IV are obtained by numerical simulation. In section V, we experimentally verify our proposed estimation scheme in a 34 Gbaud QPSK and 16-QAM systems. Finally, the conclusion is presented in section VI.

II. The Mathematical Model of Tx and Rx in the Presence of IQ Imbalance

Considering IQ imbalance is a relative relationship between I and Q channels, the signals of I channel are selected as reference and the IQ imbalances are added in the signals of Q channel for the sake of augment in the following discussion.

A. The Tx model

In Tx, the amplitude imbalance is mainly caused by non-uniform gain of the electrical amplifiers; while phase imbalance is caused by the imperfection in the phase modulator, as shown in Fig. 1. Assuming the driving signal is limited to the linear region, the output signal of Tx can be expressed as:

$$\begin{aligned} E_{Tx}(t) &\propto [S_{Tx,I}(t) + g_{Tx} S_{Tx,Q}(t) \exp(j(\pi/2 + \theta_{Tx}))] \\ &= [S_{Tx,I}(t) - g_{Tx} S_{Tx,Q}(t) \sin(\theta_{Tx}) + j g_{Tx} S_{Tx,Q}(t) \cos(\theta_{Tx})] \end{aligned}, \quad (1)$$

where $S_{Tx,I}(t)$ and $S_{Tx,Q}(t)$ represent the electrical driving signals of I and Q channels, respectively. g_{Tx} and θ_{Tx} represent the Tx amplitude and phase imbalances, respectively. The above equation can be described by the matrix equation:

$$\begin{aligned} \begin{bmatrix} E_{Tx,I}(t) \\ E_{Tx,Q}(t) \end{bmatrix} &\propto \boldsymbol{H_{Tx}} \begin{bmatrix} S_{Tx,I}(t) \\ S_{Tx,Q}(t) \end{bmatrix} \\ &= \begin{bmatrix} 1 & -g_{Tx}\sin(\theta_{Tx}) \\ 0 & g_{Tx}\cos(\theta_{Tx}) \end{bmatrix} \begin{bmatrix} S_{Tx,I}(t) \\ S_{Tx,Q}(t) \end{bmatrix}, \end{aligned} \quad (2)$$

where $E_{Tx,I}(t)$ and $E_{Tx,Q}(t)$ represent the Tx output signals of I and Q channels. $\boldsymbol{H_{Tx}}$ is defined as the Tx imbalance matrix.

B. The Rx model

In Rx, the amplitude imbalance is mainly caused by the imperfection in balanced PDs and TIAs; while the phase imbalance is caused by the imperfection in the 90 degrees optical hybrid, as shown in Fig. 2. The received electrical signal in I and Q channels can be expressed as follows:

$$\begin{aligned} S_{Rx,I}(t) &\propto \Re e(E_S(t) E_{LO}^*(t)) \\ &= A(t)\cos(\Delta\omega t + \phi_S(t) + \theta_N(t)) \end{aligned}, \quad (3)$$

$$\begin{aligned} S_{Rx,Q}(t) &\propto \Im m(g_{Rx} E_S(t) E_{LO}^*(t) \exp(j\theta_{Rx})) \\ &= A(t) g_{Rx} \sin(\Delta\omega t + \phi_S(t) + \theta_N(t) - \theta_{Rx}) \end{aligned}, \quad (4)$$

where $E_S(t)$, $E_{LO}(t)$, $A(t)$, $\phi_S(t)$, $\Delta\omega$, and $\theta_N(t)$ represent the received optical signal, local oscillator (LO) carrier, modulated amplitude, modulated phase, FO and PN, respectively. g_{Rx} and θ_{Rx} represent the Rx amplitude and phase imbalances, respectively. $\Re e$ and $\Im m$ denote the real and imaginary components of the beat products of the two light waves, respectively.

Equations (3) and (4) can also be described by the matrix equation as follows:

$$\begin{aligned} \begin{bmatrix} S_{Rx,I}(t) \\ S_{Rx,Q}(t) \end{bmatrix} &\propto A(t) \boldsymbol{H_{Rx}} \begin{bmatrix} \Re e(E_S(t) E_{LO}^*(t)) \\ \Im m(E_S(t) E_{LO}^*(t)) \end{bmatrix} \\ &= A(t) \begin{bmatrix} 1 & 0 \\ -g_{Rx}\sin(\theta_{Rx}) & g_{Rx}\cos(\theta_{Rx}) \end{bmatrix} \\ &\quad \begin{bmatrix} \cos(\Delta\omega t + \phi_S(t) + \Delta\theta(t)) \\ \sin(\Delta\omega t + \phi_S(t) + \Delta\theta(t)) \end{bmatrix}, \end{aligned} \quad (5)$$

where $\boldsymbol{H_{Rx}}$ is defined as the Rx imbalance matrix.

Essentially, estimating IQ imbalance is a process of solving the IQ imbalance matrix $\boldsymbol{H_{Tx}}$ and $\boldsymbol{H_{Rx}}$. It may be easy to individually solve $\boldsymbol{H_{Tx}}$ or $\boldsymbol{H_{Rx}}$. However, solving IQ imbalance matrix becomes difficult when $\boldsymbol{H_{Tx}}$ and $\boldsymbol{H_{Rx}}$ are mixed together.

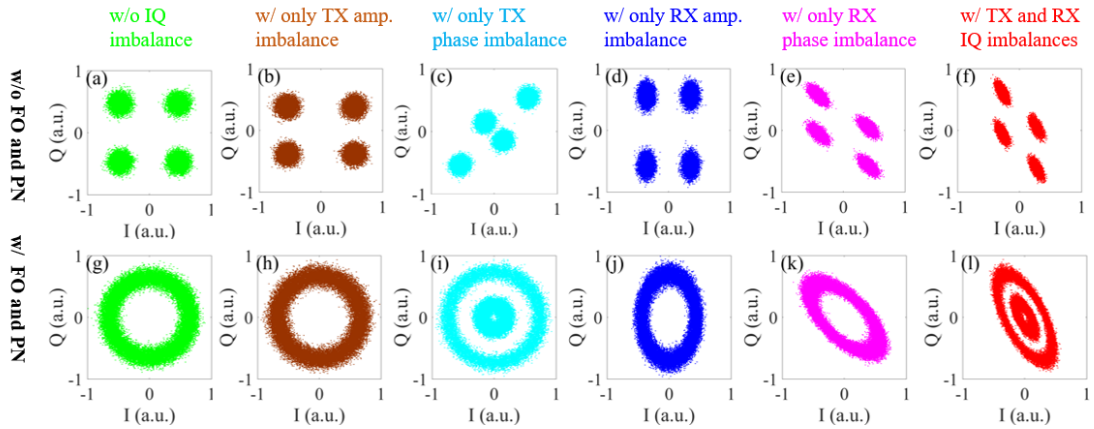

Fig. 3. The impact of IQ imbalance on the received signal constellation. The received signal constellation (a)-(f) without FO and PN, (g)-(l) with FO and PN. The received signal constellation under (a), (g) no IQ imbalance, (b), (h) Tx amplitude imbalance, (c), (i) Tx phase imbalance, (d), (j) Rx IQ amplitude imbalance, (e), (k) Rx IQ phase imbalance, (f), (l) both Tx and Rx IQ imbalance. Tx amplitude/phase imbalance is set to 3 dB/30 degrees and Rx amplitude/phase imbalance is set to 4 dB/40 degrees.

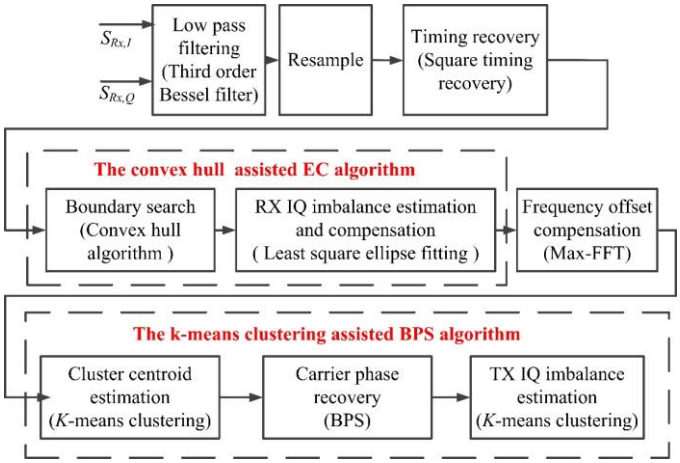

Fig. 4. The flow of the estimation scheme of IQ imbalances of Tx and Rx based on machine learning.

III. The Impact of IQ Imbalance on the Shape of the Received Signal Constellation

Both Tx and Rx IQ imbalances will distort the received signals, which may significantly degrade the system performance, as shown in Fig. 3. In this and subsequent section, symbol rate, FO, and PN are set to 34 Gbaud, 1 GHz, and 100 KHz in numerical simulation, respectively. In absence of FO and PN, the amplitude and phase imbalances cause the constellation to change from a square to a rectangle and a parallelogram, respectively, as shown in Fig. 3(a)-(f). In this case, it is difficult to distinguish whether the distortion comes from Tx or Rx. However, FO and PN always exist in a practical system, which makes it possible to distinguish between Tx and Rx imbalances from the constellations, as shown in Fig. 3(g)-(l). Tx phase imbalance will cause the constellation to become a concentric circle, as shown in Fig. 3(i). Rx imbalance will cause the constellation to change from a circle to an ellipse, as shown in Fig. 3(j)-(l). It is easy to find that the Rx IQ imbalance is the only factor which makes the received signal constellation to change from a circle to an ellipse. In view of the obvious characteristics of the constellation, it is a natural idea to estimate both Tx and Rx imbalances according to the constellation. In the following section, the detailed principle is introduced.

IV. Blind and Separate Estimation of Tx and Tx IQ Imbalances

Fig. 4 shows the overall flow of the proposed scheme. After timing recovery [15], a convex hull assisted ellipse correction (EC) algorithm is used to determine the Rx IQ imbalance parameters that best match the ellipses. The Rx IQ imbalances are then compensated. Standard laser FO compensation algorithm [16] follows. A *k*-means clustering assisted blind phase search (BPS) algorithm is then employed to mitigate the PN in presence of Tx imbalances. Finally, another iterative *k*-means clustering procedure is used to estimate the Tx IQ imbalances. The details of the proposed estimating procedures are as follows.

A. Estimation of Rx IQ imbalance

EC is a classical algorithm to fit an ellipse based on the LS criteria. Considering Rx IQ imbalance causes the constellation of constant modulus signals to become an ellipse, then EC algorithm can be used to estimate and compensate the Rx IQ imbalance, as shown in Fig. 5(a). However, it would not work when multiple circles exist in the received constellation diagrams, which is the case for multi-modulus signals, or QPSK signals with Tx IQ imbalance. For QPSK signals with both Rx and Tx IQ imbalances [as shown in Fig. 5(b)], or 16QAM signals with Rx IQ imbalance [as shown in Fig. 5(c)], or 16QAM signals with Rx and Tx IQ imbalance [as shown in Fig. 5(d)], the conventional EC algorithm failed to work.

To address this problem, we propose a convex hull assisted EC algorithm to estimate the Rx IQ imbalance. The flow of the proposed algorithm is as follows: firstly, a convex hull algorithm is used to find the samples on the constellation boundary; then LS ellipse fitting is used in these signals to find the LS ellipse; finally Rx IQ imbalances are estimated based on the parameters of the LS ellipse equation. The convex hull algorithm is a kind of classical algorithm in computational geometry and can be used to find the contour of a figure [18]. Some boundary signals can be obtained by using convex hull

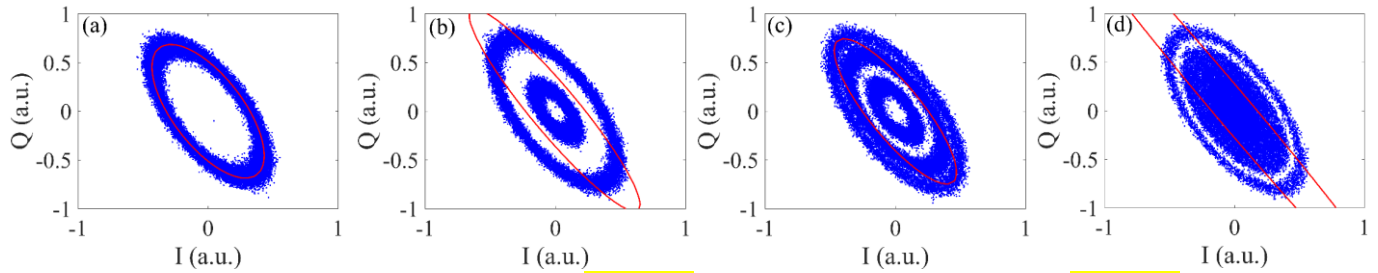

Fig. 5. The fitting curve obtained by the EC algorithm in (a) QPSK constellation in presence of Rx IQ imbalance (b) QPSK constellation in presence of both Tx and Rx IQ imbalances (c) 16-QAM constellation in presence of Rx IQ imbalance (d) 16-QAM constellation in presence of both Tx and Rx IQ imbalances. The blue points represent the received signal. The red curve represents the fitting ellipse.

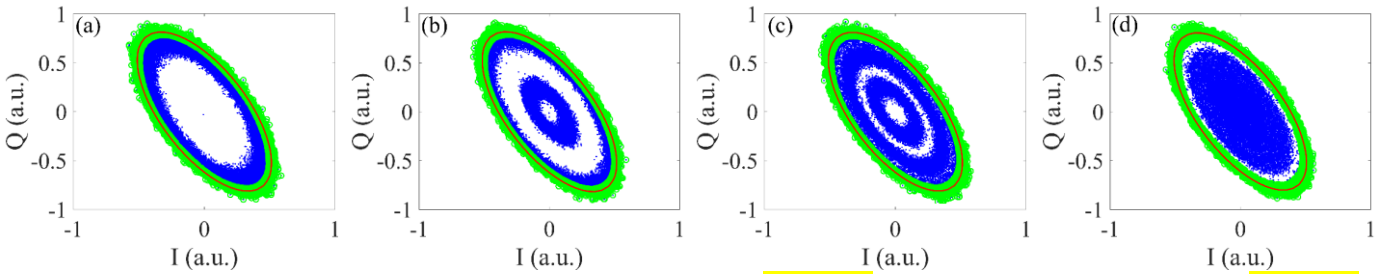

Fig. 6. The fitting curve obtained by the convex hull assisted EC algorithm in (a) QPSK constellation in presence of Rx IQ imbalance (b) QPSK constellation in presence of both Tx and Rx IQ imbalances (c) 16-QAM constellation in presence of Rx IQ imbalance (d) 16-QAM constellation in presence of both Tx and Rx IQ imbalances. The blue points represent the received signal, the green points represent the boundary signals, and the red curve represents the fitting ellipse.

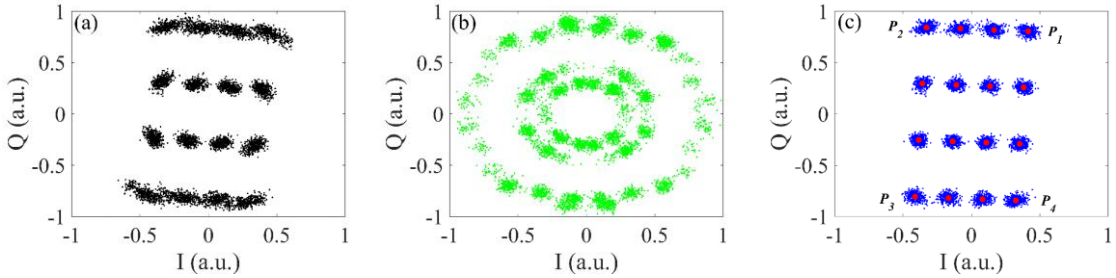

Fig. 7. The constellation (a) without phase recovery (b) with BPS, and (c) with k-means assisted BPS for 16-QAM signal under 7 dB Tx amplitude imbalance in one block. Red circular makers represent cluster centroid.

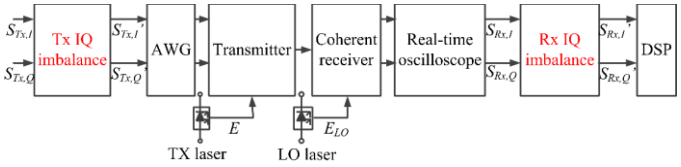

Fig. 8. Block diagram of the experimental setup.

algorithm and the remainder signals are used in next convex hull algorithm to obtain new boundary signals. In this way, new boundary signals can be obtained each time the convex hull algorithm is used. In our scheme convex hull algorithm is used 50 times to obtain enough boundary signals for fitting the LS ellipse. As shown in Fig. 6(b), although Tx IQ imbalance causes the QPSK constellation to change from single ellipse to multiple ellipses, the boundary signals can be extracted by the convex hull algorithm. The convex hull algorithm also works in 16-QAM signals with IQ imbalances, as shown in Fig. 6(c)-(d). Note that the Tx IQ imbalance has no impact on the contour of the constellation. Therefore, the convex hull assisted EC algorithm can be used to estimate the Rx IQ imbalance in presence of Tx IQ imbalance for constant and multiple modulus signals. When the boundary signals are found, the LS ellipse can be obtained. As shown in Fig 6(b)-(d), the fitting ellipse consistent with the constellation boundary are found by the modified EC algorithm for QPSK and 16-QAM systems in presence of Tx and Rx IQ imbalance.

After the LS ellipse is obtained, the Rx IQ imbalance can be estimated according to the parameters of the ellipse equation. The LS ellipse equation can be expressed as follows:

$$\begin{aligned} &aS_{Rx,I}{}^2(t)+bS_{Rx,I}(t)S_{Rx,Q}(t)+cS_{Rx,Q}{}^2(t) \\ &+dS_{Rx,I}(t)+eS_{Rx,Q}(t)-\Delta=0 \end{aligned}, \quad (6)$$

where a, b, c, d, and e are the coefficients of ellipse equation and Δ is a constant.

According to (5):

$$g_{Rx}^2 S_{Rx,I}{}^2(t)+2g_{Rx}\sin(\theta_{Rx})S_{Rx,I}(t)S_{Rx,Q}(t)+S_{Rx,Q}{}^2(t)-1=0 \quad . \quad (7)$$

g_{Rx} and θ_{Rx} can be obtained by solving (8) and (9):

$$g_{Rx}=\sqrt{a/c} \ , \quad (8)$$

$$\theta_{Rx}=\arcsin(b/2g_{Rx}c) \ . \quad (9)$$

B. Estimation of Tx IQ imbalance

PN causes the crosstalk between I and Q channels. Therefore,

PN should be compensated firstly in order to estimate the Tx IQ

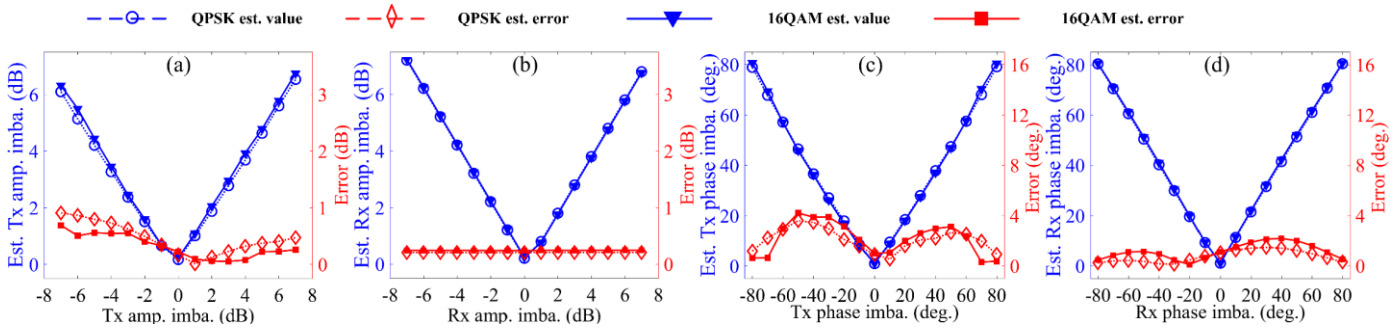

Fig. 9. The estimation of IQ imbalance in the presence of only one kind of IQ imbalance for QPSK and 16-QAM. Estimation of (a) Tx IQ amplitude imbalance, (b) Rx IQ amplitude imbalance, (c) Tx IQ phase imbalance, and (d) Rx IQ phase imbalance.

imbalance. BPS is a popular phase compensation algorithm, which uses the test phase to mitigate the PN [19]. However, IQ imbalance may cause BPS to make the wrong signal decision and subsequently implement erroneous phase compensation. This phenomenon is depicted in Fig. 7, where a 7 dB Tx IQ amplitude imbalance is introduced to the 34 Gbaud 16-QAM signal with an optical signal-to-noise ratio (OSNR) of 26 dB. One can see from Fig. 7(b) that apparently BPS does not work in this scenario; since the standard 16-QAM constellation can not be used here as a reference for signal detection due to the presence of the amplitude imbalance. Therefore, we propose a *k*-means clustering assisted BPS algorithm to improve the performance of phase compensation before Tx IQ imbalance estimation. *K*-means algorithm is a popular clustering algorithm and widely used in data mining and pattern recognition. According to the principle of minimum Euclidean distance, the algorithm iteratively partitions the clusters and calculates the cluster centroid coordinates. In the proposed scheme, a *k*-means clustering algorithm is firstly introduced to find the cluster centroids before BPS. Then the obtained cluster centroids are used as the constellation reference in BPS to avoid wrong decision. The recovered signals by BPS are sent back to a second *k*-means clustering procedure for Tx IQ imbalance estimation. Fig. 7(c) shows the recovered constellation using our proposed method. Obviously, the carrier phase is correctly compensated with the help of the new reference constellation obtained via the *k*-means clustering algorithm.

Since Tx IQ imbalance and phase ambiguity will change the shape of the constellation, the relative position of cluster centroid should be determined. The distances between each two centroids are calculated for determining the relative position of centroids. The two centroids which have the farthest distance are defined as P_1 and P_2 and the farthest two points from P_1P_2 are defined as P_3 and P_4, as shown in Fig. 7(c). The above four centroids can be used to calculate the Tx IQ imbalance by the following equations:

$$g_{Tx} = |P_1P_2| / |P_2P_3|, \tag{10}$$

$$\theta_{Tx} = \pi/2 - arc\cos((|P_1P_2|^2 + |P_2P_3|^2 - |P_1P_3|^2) / 2|P_1P_2||P_2P_3|). \tag{11}$$

V. Experimental Verifications

The experimental setup is shown in Fig. 8. 34 Gbaud electrical signals were generated using a pseudo-random bit sequence (PRBS) of length 2^{15}-1. After QPSK/16-QAM mapping, the modulated signals were then spectral shaped using a root raised cosine (RRC) filter with a roll-off factor of 0.3, pre-distorted to introduce the Tx imbalances, and then sent to an arbitrary waveform generator (AWG, Keysight M8196A) with a sampling rate of 85-GS/s. The generated electrical signals were amplified and sent to drive an optical I/Q modulator (Fujitsu FTM7962EP). An external cavity laser (ECL N7714A) with a central wavelength of 1550.12 nm was used as the optical carrier. The modulated optical signals were then sent directly to a coherent receiver (Fujitsu FIM24706EB). Subsequently, the detected electrical signals are sampled by a real-time oscilloscope (Agilent DSA-X-96204Q) at 80 GS/s. It should be noted that the IQ imbalances are introduced digitally in the Tx and Rx DSP, since it is difficult to add precise IQ imbalances by controlling the electrical and optical devices. This process can be expressed by the following equations:

$$\begin{bmatrix} S_{Tx,I}'(t) \\ S_{Tx,Q}'(t) \end{bmatrix} = \boldsymbol{H_{Tx}} \begin{bmatrix} S_{Tx,I}(t) \\ S_{Tx,Q}(t) \end{bmatrix} = \begin{bmatrix} S_{Tx,I}(t) - g_{Tx}S_{Tx,Q}(t)\sin(\theta_{Tx}) \\ g_{Tx}S_{Tx,Q}(t)\cos(\theta_{Tx}) \end{bmatrix}, \tag{12}$$

$$\begin{bmatrix} S_{Rx,I}'(t) \\ S_{Rx,Q}'(t) \end{bmatrix} = \boldsymbol{H_{Rx}} \begin{bmatrix} S_{Rx,I}(t) \\ S_{Rx,Q}(t) \end{bmatrix} = \begin{bmatrix} S_{Rx,I}(t) \\ -g_{Rx}S_{Rx,I}(t)\sin(\theta_{Rx}) + g_{Rx}S_{Rx,Q}(t)\cos(\theta_{Rx}) \end{bmatrix}. \tag{13}$$

In our experimental implementation, the received signals are divided into blocks with a length of 1500. The convex hull algorithm is used 50 times to find enough boundary signals. The sliding window and the number of test phases are set to 50 and 64 in BPS, respectively. The native IQ imbalance of experimental system is tested by the commercial software (Keysight 89600 VSA) with the relatively small values of less than 0.5 dB and 1 degree for amplitude and phase imbalance. Therefore, it is reasonable to consider the digitally introduced IQ imbalance in Tx and Rx as reference to evaluate the

estimation accuracy

Firstly, we experimentally investigate the estimation performance of the proposed algorithm for both QPSK and 16-QAM signals when only one of the four imbalances (Tx amplitude imbalance, Tx phase imbalance, Rx amplitude imbalance, and Rx phase imbalance) exists. The results are

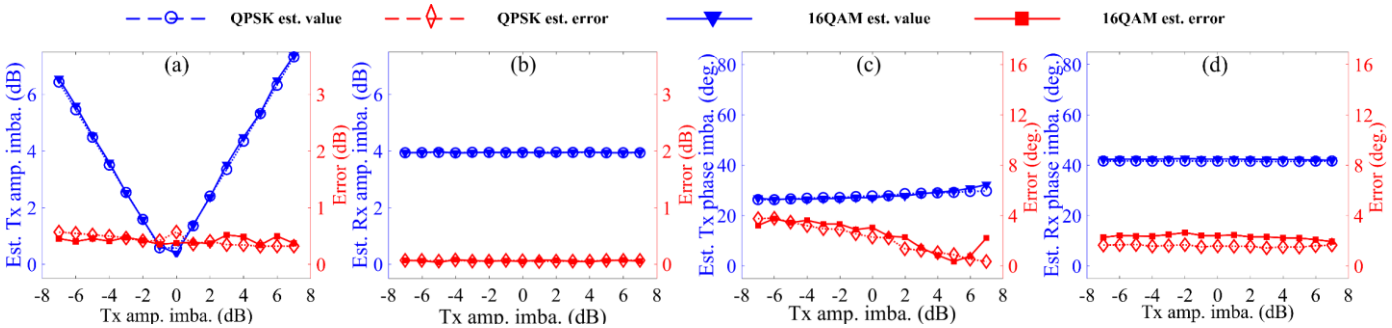

Fig. 10. The estimation of IQ imbalance under different Tx amplitude imbalances in the presence of 30 degrees Tx phase imbalance and 4 dB/40 degrees Rx amplitude/phase imbalance for QPSK and 16QAM. Estimation of (a) Tx IQ amplitude imbalance, (b) Rx IQ amplitude imbalance, (c) Tx IQ phase imbalance, and (d) Rx IQ phase imbalance.

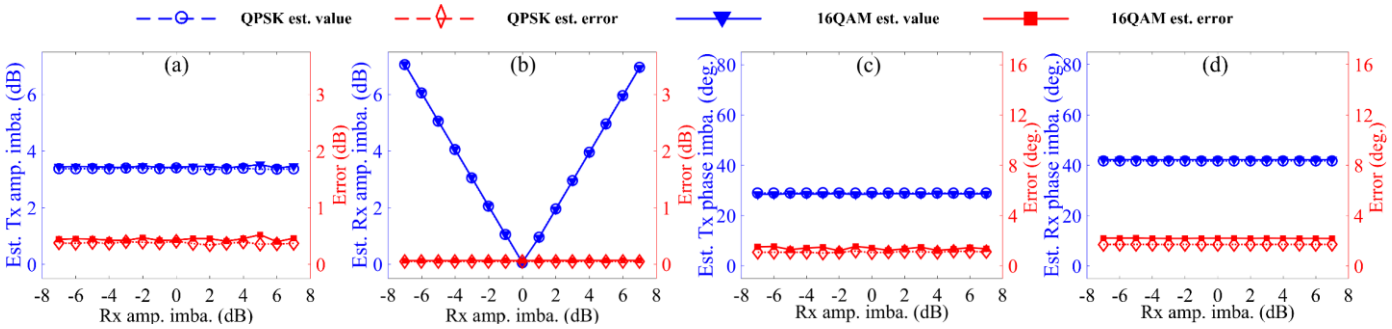

Fig. 11 The estimation of IQ imbalance under different Rx amplitude imbalances in the presence of 40 degrees Rx phase imbalance and 3 dB/30 degrees Tx amplitude/phase imbalance for QPSK and 16-QAM. Estimation of (a) Tx IQ amplitude imbalance, (b) Rx IQ amplitude imbalance, (c) Tx IQ phase imbalance, and (d) Rx IQ phase imbalance.

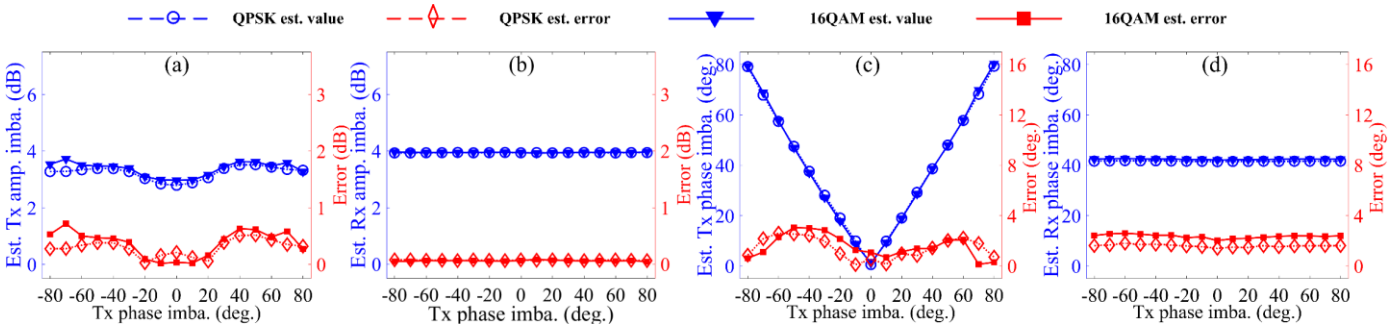

Fig. 12 The estimation of IQ imbalance under different Tx phase imbalances in the presence of 3 dB Tx phase imbalance and 4 dB/40 degrees Rx amplitude/phase imbalance for QPSK and 16-QAM. Estimation of (a) Tx IQ amplitude imbalance, (b) Rx IQ amplitude imbalance, (c) Tx IQ phase imbalance, and (d) Rx IQ phase imbalance.

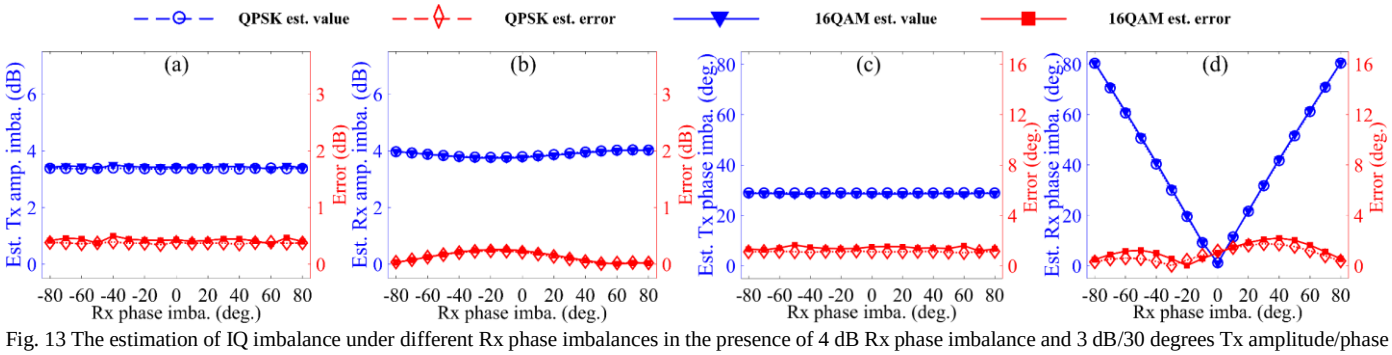

Fig. 13 The estimation of IQ imbalance under different Rx phase imbalances in the presence of 4 dB Rx phase imbalance and 3 dB/30 degrees Tx amplitude/phase imbalance for QPSK and 16-QAM. Estimation of (a) Tx IQ amplitude imbalance, (b) Rx IQ amplitude imbalance, (c) Tx IQ phase imbalance, and (d) Rx IQ phase imbalance.

shown in Fig. 9. For QPSK and 16-QAM, the estimation ranges of Tx and Rx amplitude imbalances are -7 dB to 7 dB within 1 dB of estimation error. The estimation ranges of Tx and Rx phase imbalances are -80 degrees to 80 degrees within 4 degrees of estimation error. The experiment results demonstrate that the proposed scheme can accurately estimate the Tx or Rx IQ

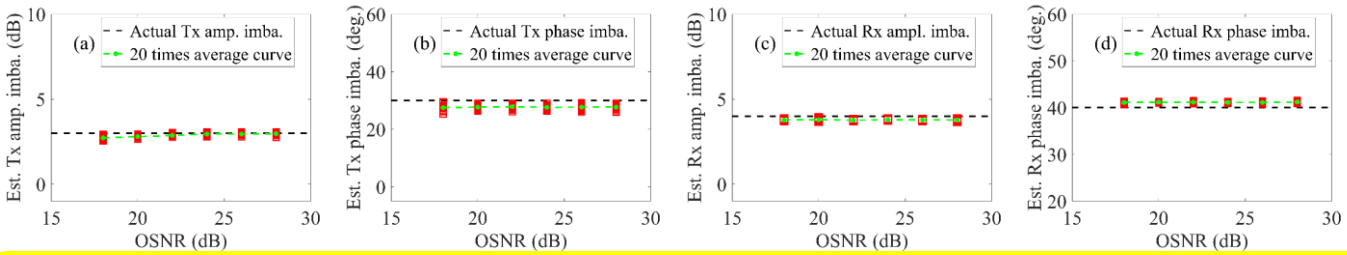

Fig. 14. The estimation of IQ imbalance under different OSNR for 16-QAM signals. Estimation of (a) Tx IQ amplitude imbalance, (b) Rx IQ amplitude imbalance, (c) Tx IQ phase imbalance, and (d) Rx IQ phase imbalance. The green circular dots are calculated by averaging 20 sets of data; The red square boxes are calculated by one set of data; The black dotted lines represent actual IQ imbalance.

TABLE I
PARAMETER SETTINGS OF JOINT Tx AND Rx IMBALANCE ESTIMATION FOR QPSK AND 16QAM SYSTEMS

Mod. Formats	Scenario	Tx Amp. Imba. (dB)	Rx Amp. Imba. (deg.)	Tx Phase Imba. (dB)	Rx Phase Imba. (deg.)
QPSK/ 16QAM	1	-7 to 7	30	4	40
	2	3	-80 to 80	4	40
	3	3	30	-7 to 7	40
	4	3	30	4	-80 to 80

imbalances within a wide range in presence of only one kind of IQ imbalance. It is noteworthy that the estimation accuracy of Rx imbalance is higher than that of Tx imbalance. Because the estimation accuracy of Tx imbalance is limited by the FO and PN. Unfortunately, the performance of conventional compensation algorithms of FO and PN will be degraded by Tx imbalance. Further discussion on these algorithms, however, is out of scope of this paper.

Secondly, the performance of our proposed algorithm is extensively investigated when both Tx and Rx IQ imbalances are present. During each run, only one of the four impairments is adjusted in a wide range while the other three were fixed with a proper value. The parameters used for the experiments are showed in TABLE I. Four kinds of scenarios are tested in our experiment. In the scenario 1, four kinds of IQ imbalances are estimated under different Tx amplitude imbalances, as shown in Fig. 10. The results demonstrate that the proposed algorithm can accurately estimate Tx amplitude imbalance within a wide range in presence of other IQ imbalances and maintain good estimation performance for Rx IQ imbalances with the change of Tx amplitude imbalance. The estimation performance of Tx phase imbalance has 2 degrees of degradation with the Tx amplitude imbalance changed from 0 to 8 dB. In the scenario 2, the IQ imbalances are estimated under different Rx amplitude imbalances, as shown in Fig. 11. The results show that the proposed algorithm can accurately estimate Rx amplitude imbalance within a wide range in presence of other IQ imbalances and keep good estimation performance for other three kinds of IQ imbalances even with the adjusted Rx amplitude imbalance. In the scenario 3, the IQ imbalances are estimated under different Tx phase imbalances, as shown in Fig. 12. The results show that the proposed algorithm can accurately estimate Tx phase imbalance within a wide range in presence of other IQ imbalances and also keep good estimation performance for Rx IQ imbalances with the change of Tx phase imbalance. The estimation performance of Tx amplitude imbalance has 0.5 dB of degradation with the Tx phase imbalance changed from 0 to 80 degrees. In the scenario 4, the IQ imbalances are estimated under different Rx phase imbalances, as shown in Fig. 13. The results show that the proposed algorithm can accurately estimate Rx phase imbalance within a wide range in presence of other IQ imbalances and have good estimation performance for other three kinds of IQ imbalances under the tuned Rx amplitude imbalance. Therefore, the proposed algorithm has wide estimation range and excellent estimation accuracy when the amplitude and phase imbalances of both Tx and Rx exist at the same time.

Finally, the proposed scheme is investigated under different OSNR. At each OSNR 20 data sets are collected and the sample length of each sampled data set is 200,000. The Tx/Rx amplitude and phase imbalances are set to 3/4 dB and 30/40 degrees, respectively. As shown in Fig. 14, the proposed scheme has stable estimation performance within wide OSNR range. The estimated bias and variance of phase imbalance are less than 3 degrees and 1 degree, respectively. The estimated bias and variance of amplitude imbalance are less than 0.3 dB and 0.02 dB, respectively. Therefore, it's confirmed that the proposed algorithm has strong robustness to ASE noise and can be used for analyzing the degraded signal by ASE after transmission.

VI. Conclusion

We have proposed a blind, wide-range IQ imbalance estimation scheme capable of estimating imbalances from both Tx and Rx separately in coherent optical systems by employing a mixture of analytical modelling and clustering algorithms. We

have experimentally evaluated the proposed scheme in QPSK and 16-QAM modulated coherent systems. It has been proved that the proposed algorithm is applicable to estimate the IQ imbalances of both Tx and Rx within a wide range for both constant and multi-modulus modulation format and has strong robustness to ASE noise. The proposed algorithm can respectively estimate Tx and Rx amplitude IQ imbalances ranged from -7 dB to 7 dB within 1 dB of estimation error for QPSK and 16-QAM. The proposed algorithm can respectively estimate Tx and Rx phase IQ imbalances ranged from -80 degrees to 80 degrees within 4 degrees of estimation error for QPSK and 16-QAM. The proposed scheme has a wide application potential for characterizing and diagnosing transceivers modules for network disaggregation applications.

REFERENCES

[1] T. H. Nguyen et al., "Blind transmitter IQ imbalance compensation in M-QAM optical coherent systems," *J. Opt. Commun. Netw.*, vol. 9, no. 9, pp. D42-D50, Sep 2017.

[2] T. H. Nguyen et al., "Blind adaptive transmitter IQ imbalance compensation in M-QAM optical coherent systems," in Proc. *IEEE International Conference on Communications (ICC)*, Kuala Lumpur, pp. 1-6, 2016.

[3] M. S. Faruk and K. Kikuchi, "Compensation for in-phase/quadrature imbalance in coherent-receiver front end for optical quadrature amplitude modulation," *IEEE Photon. J.*, vol. 5, no. 2, pp. 7800110-7800110, Apr 2013.

[4] I. Fatadin, S. J. Savory and D. Ives, "Compensation of quadrature imbalance in an optical QPSK coherent receiver," *IEEE Photon. Technol. Lett.*, vol. 20, no. 20, pp. 1733-1735, Oct 2008.

[5] S. H. Chang, H. S. Chung and K. Kim, "Impact of quadrature imbalance in optical coherent QPSK receiver," *IEEE Photon. Technol. Lett.*, vol. 21, no. 11, pp. 709-711, Jun 2009.

[6] R. Rios-Müller, J. Renaudier and G. Charlet, "Blind receiver skew compensation and estimation for long-haul non-dispersion Managed Systems Using Adaptive Equalizer," *J. Lightwave Technol.*, vol. 33, no. 7, pp. 1315-1318, Apr 2015.

[7] M. Faruk and S. Savory, "Digital signal processing for coherent transceivers employing multilevel formats," *J. Lightwave Technol.*, vol. 35, no. 5, pp. 1125–114, 2017

[8] E. P. da Silva and D. Zibar, "Widely linear equalization for IQ imbalance and skew compensation in optical coherent receivers," *J. Lightwave Technol.*, vol. 34, no. 15, pp. 3577-3586, Aug 2016.

[9] T. H. Nguyen et al., "Joint simple blind IQ imbalance compensation and adaptive equalization for 16-QAM optical communications," in Proc. *IEEE International Conference on Communications (ICC)*, London, pp. 4913-4918, 2015.

[10] W. Nam, H. Roh, J. Lee and I. Kang, "Blind adaptive I/Q Imbalance compensation algorithms for direct-conversion receivers," *IEEE Signal Process. Lett.*, vol. 19, no. 8, pp. 475-478, Aug 2012.

[11] M. Valkama, M. Renfors and V. Koivunen, "Blind signal estimation in conjugate signal models with application to I/Q imbalance compensation," *IEEE Signal Process. Lett.*, vol. 12, no. 11, pp. 733-736, Nov 2005

[12] C.R.S. Fludger, T. Kupfer, "Transmitter impairment mitigation and monitoring for high baud-rate, high order modulation systems" in Proc. *European Conference on Optical Communication (ECOC)*, Dusseldorf, pp. 256-258, 2016.

[13] H. S. Chung, S. H. Chang and K. Kim, "Effect of IQ mismatch compensation in an optical coherent OFDM receiver," *IEEE Photon. Technol. Lett.*, vol. 22, no. 5, pp. 308-310, Mar 2010.

[14] M. I. Khalil, A. M. Chowdhury and Gee-Kung Chang, "Efficient FIR filter configuration to joint IQ imbalance and carrier-phase recovery in 16-QAM coherent receivers," in Proc. *Conference on Lasers and Electro-Optics (CLEO) - Laser Science to Photonic Applications*, San Jose, CA, pp. 1-2, 2014.

[15] M. Oerder and H. Meyr, "Digital filter and square timing recovery," *IEEE Trans. Commun.*, vol. 36, no. 5, pp. 605-612, May 1988.

[16] M. Selmi, Y. Jaouen and P. Ciblat, "Accurate digital frequency offset estimator for coherent PolMux QAM transmission systems," in Proc. *European Conference on Optical Communication*, Vienna, pp. 1-2, 2009.

[17] A. Fitzgibbon, M. Pilu and R. B. Fisher, "Direct least square fitting of ellipses," *IEEE Trans. Pattern Anal. Mach. Intell.*, vol. 21, no. 5, pp. 476-480, May 1999.

[18] J. Zhang, X. Lu, K. C. Chou, Y. A. Chang, "Application of Graham scan algorithm in binary phase diagram calculation" *J. Phase Equilib. Diffus.*, vol. 27, no. 2, pp 121-125, Mar 2006.

[19] T. Pfau, S. Hoffmann and R. Noe, "Hardware-efficient coherent digital receiver concept with feedforward carrier recovery for M -QAM Constellations," *J. Lightwave Technol.*, vol. 27, no. 8, pp. 989-999, Apr 2009